Available online at www.eccomasproceedia.org
Eccomas Proceedia SMART (2023) 1507-1518

ECCOMAS
Proceedia

X ECCOMAS Thematic Conference on Smart Structures and Materials
SMART 2023
D.A. Saravanos, A. Benjeddou, N. Chrysochoidis and T. Theodosiou (Eds)

ACTIVELY RESPONSIVE ANISOTROPIC MULTILAYER MATERIALS AS ACTUATORS

GRIGORIOS M. CHATZIATHANASIOU[1,2*], NIKOLAOS ATHANASOPOULOS[1*]

[1]Foundation for Research and Technology Hellas,
Institute of Chemical Engineering Sciences, Patras, Greece, Stadiou str., Platani, 26504
*email: n.athanasopoulos@iceht.forth.gr, athanasopoulos@4d-mater.com,
nikos_athanasopoulos@protonmail.com

[2]Department of Mechanical Engineering & Aeronautics, University of Patras, 26504, Greece
*email: chatziathanasiou@iceht.forth.gr, chatziathanasiou.g@upnet.gr

Abstract. In Nature, it is common for dead tissues to consist of materials with anisotropic multilayer and non-homogenous or bistable structures. The structure determines their self-shaping and self-folding capabilities in response to a stimulus in order to activate different functionalities. In this research activity, we present a low-cost actuator, comprising of an anisotropic highly oriented polyethylene layer and a copper network, connected with a thin adhesive. Small temperature alterations due to Joule heating yield high out-of-plane movement, due to the extremely high mismatch in the coefficient of thermal expansion. An experimental campaign revealed the temperature-dependent material properties of the polyethylene, which were consecutively used in high-fidelity finite element (FE) models to find the appropriate-for-actuation polyethylene thickness. The performance of the actuator was examined experimentally and numerically, revealing high displacements and rotations for small temperature changes, therefore high sensitivity appears. The actuators could find applications in Space industry and electronics where the weight and volume reduction are imperative.

Key words: Responsive Multilayer Materials, Thermomechanical Coupling, Soft Actuators, Bioinspired actuators, electrothermal actuators

1 INTRODUCTION

In Nature, numerous plants and dead tissues of plants use their anisotropic properties, heterogeneity and their multilayer structure in order to achieve complex movements [1] and survive under dynamic environment. Using layer-by-layer manufacturing techniques and other fabrication processes such as laser patterning, etching, we can re-create materials with specific structure that are responsive to a variety of external stimuli (terms such as, stimuli-responsive materials, active materials, self-shape materials have been also coined). Bi-morphs and other bilayer or multilayer strategies have been used in order to fabricate actuators for a plethora of applications [2,3]. These bio-inspired actuators have expanded their application boundaries showing promising advantages in soft robotics, morphable electronics, biomedicine and thermal control for Space and architecture [2-8]. Using programmable protocols, we can control

© 2023 The Authors. Published by Eccomas Proceedia.
Peer-review under responsibility of the organizing committee of SMART 2023.
doi: 10.7712/150123.9922.452848

locally the material properties and therefore the geometry and shape-change response of the actuator. All in all, controlling the anisotropy, heterogeneity, and adding layers, we can fabricate stimuli-responsive materials using various combinations. Representative responsive materials that can be used as bioinspired actuators include hydrogels, liquid crystals, pre-stretched layers, vapomechanically responsive polymers, shape memory polymers, magnetic hydrogels and other composite materials [2-7]. The unlimited combinations of the materials and their structure formation, could lead to extreme shape-changing capabilities that can be used in various sectors and applications.

Anisotropic and heterogenous monolayers and multilayers could form complex shapes. In any case, the shape change occurs by introducing mismatch strain through the thickness of the materials/structures [2,3]. For example, stimuli–responsive hydrogels changing their volume and their shape through swelling in response to humidity [5]. Also, hydrogels with magnetically aligned nano-particles have been also studied [4]. Also, the development of soft electrothermal actuators has attracted the engineering community. These soft actuators can be used in soft robots, manipulators, variable shading [8], and radiative thermal management [9,10]. Comparing various soft actuators, electrothermal actuators show better performance in large deformation, fast response, weight, fabrication simplicity, as well as low driving voltage [8]. A soft electrothermal actuator is composed of at least two layers with a great difference in coefficient of thermal expansion (CTE). When an electrical voltage is applied, the conductive layer with a lower CTE generates heat (Joule heating effect) and increases the temperature of the whole actuator. Due to the multilayer structure and its anisotropic properties, as well as induced heterogeneities, we can control the shape deformation of the actuator. According to the literature, the high efficiency of electrothermal conversion is a key. Speeding up the response during heating and cooling in a full cycle is imperative. Finally, the applied voltage should be as low as possible by decreasing the resistance of the conductive heating network. If the repeatability of the actuator and the stability of the materials is achieved, then the industry could implement them in various sectors.

In order to optimize the performance, materials with very high coefficient of expansion are required, as well as conductive networks with high thermal conductivity. In this study, we have developed and studied, anisotropic multilayer actuators using a hybrid strategy. Therefore, the proposed actuator consists of highly oriented High-Density Polyethylene (HDPE) and copper networks. We investigated the CTE of the oriented HDPE as a function of temperature and we studied the performance experimentally and numerically.

2 MATERIALS AND METHODS

The fabricated multilayer responsive materials are consisted of at least two layers and an ultrathin adhesive for low surface energy plastics (<10μm). We selected thin and thick films of oriented HDPE which presents anisotropic CTE properties. Then we formed copper networks in order to control the anisotropy and allow the activation through electrical voltage. We measured the CTE of the HDPE in two principal axis 0^o and 90^o, in order to investigate the response of the expansion and contraction as a function of temperature. Then, we used the geometrically non-linear coupled temperature-displacement loading step thermomechanical model of ABAQUS incorporating our temperature-dependent material properties and predicted

the final shape of the actuator as a function of temperature or the applied electrical power. Also, an actuator with specific geometry was fabricated in order to study its performnce. Finally, a gripper was modeled in ABAQUS in order to lift a rectangular plate.

2.1. Materials and manufacturing

An HDPE film with 125μm of thickness was purchased from R&G. Copper foil of 40μm was used for the conductive networks, while an ultrathin adhesive was used to join the different layers. The formation of the conductive network was established using masks, laser scrubbing and etching techniques. The final actuator is presented in Figure 1. For the activation we attached a commercial connector.

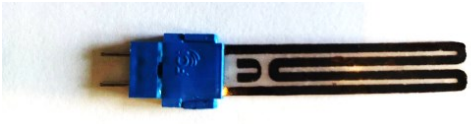

Figure 1: Representative multilayer electrothermal actuator.

2.2. Governing Equations of the thermo-mechanical problem

The actuator of Fig. 1, was modelled using electro-thermo-mechanical as a plain-strain problem, as well as a 3D problem. The electrical heat flux (Q_{el}) is calculated through the well-known Eq. 1 (Joule heating).

$$Q_{el} = J \cdot E \qquad (1)$$

Steady-state as well as transient models were built for the accurate modelling of the actuator in order to predict the shape-change. A coupled thermo-mechanical and geometrically non-linear problem was solved. The strain tensor implements also large rotations as well as temperature-dependent material properties, Eq. 2.

$$e_{el} = \frac{1}{2}\left[(\nabla u)^T + \nabla u + (\nabla u)^T \nabla u\right] - a_{(T)}\left(T - T_{ref}\right) \qquad (2)$$

The $CTE_{(T)}$ curve can be fitted/represented by Boltzmann fitting curve in order to implement the temperature dependence. The modulus of elasticity $E_{(T)}$ is also a function of temperature, and both parameters are dominant and affect significantly the final solution.

The CTE ($\alpha_{(T)}$) of the oriented HDPE is expressed by a 2nd order tensor (α), because of its anisotropic characteristics in terms of CTE. In the principal axes, the tensor is given by Eq. 3.

$$\alpha_{(T)} = \begin{bmatrix} \alpha_{11(T)} & 0 & 0 \\ 0 & \alpha_{22(T)} & 0 \\ 0 & 0 & \alpha_{33} \end{bmatrix} \qquad (3)$$

The plane-strain problem omits the $\alpha_{22(T)}$ (in-plane coefficient), while the $\alpha_{33(T)}$ that represents the through thickness CTE) assumed to be constant and equal to 200μm/m^{o}C (CTE value for bulk HDPE). However, the 3D model requires all coefficients of thermal expansion. Hence, the 3D model implements the $\alpha_{11(T)}$, $\alpha_{22(T)}$ as a function of temperature and α_{33} a constant value.

Because of the anisotropy and the local heterogeneities of the oriented HDPE, we decided

to study the behaviour of the material using large specimens, at two main principal axes. An apparatus (temperature-controlled heating chamber) was manufactured and we measured the displacement using a laser measurement setup. We examined three samples as a function of temperature. This specific apparatus was manufactured in order to assure uniform temperature distribution along the specimen. Four thermocouples were used in order to assure the temperature uniformity. The displacement due to the expansion of the film was measured using a high precision laser of 1μm accuracy. Consequently, we calculated the CTE as a function of temperature during the expansion phase, as well as during the shrinkage phase, which alters the dimensions of the film significantly. Using the Boltzmann fitting curve, we observe a very good match for each curve for the entire temperature span. However, we observe large discrepancies in the contraction of the film.

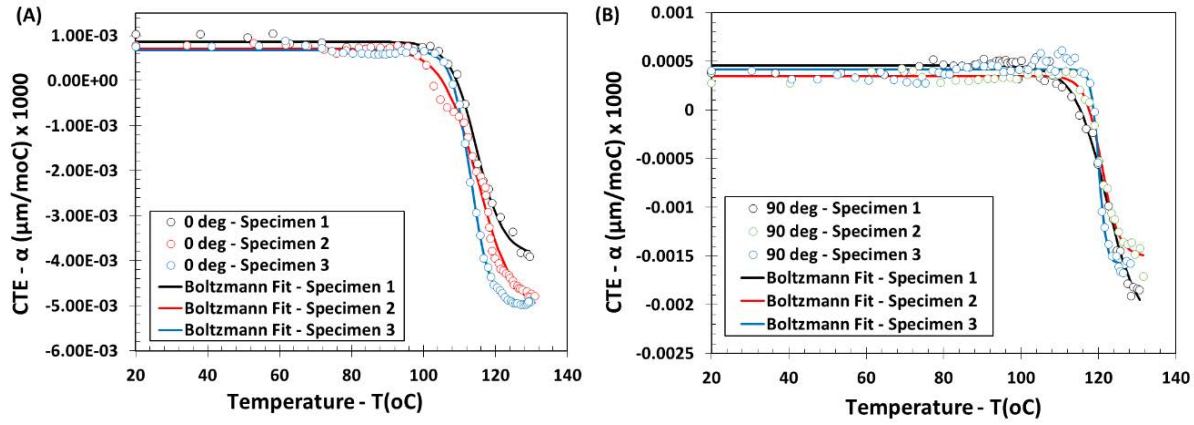

Figure 2: (A) CTE measurements of HDPE films at 0°, (B) CTE measurements of HDPE films at 90°.

Boltzmann fitting formulas is given by Eqs. 4. All necessary parameters of Table 1 are required in order to draw the Boltzmann fitting curve, and are given in the following table for replication purposes. Using these values, two CTE curves can be implemented into the FE models ($\alpha_{11(T)}$ α_{33} for the 2D model, and $\alpha_{11(T)}$ $\alpha_{22(T)}$ α_{33} for the 3D model).

$$\alpha_{11(T)} = \frac{A_1 - A_2}{1 + e^{(T - x_o)/dx}} + A_2, \qquad \alpha_{22(T)} = \frac{A_1' - A_2'}{1 + e^{(T - x_o')/dx'}} + A_2' \quad (4)$$

Table 1. Fitting parameters of CTE $\alpha_{11(T)}$ and CTE $\alpha_{22(T)}$, according to Boltzmann formulas (Eq. 4), and fitting parameters of the modulus (E) using an exponential function, Eq. 5.

A_1	7.46E-04	**A_1'**	4.02E-04	**B_1**	1.009 E9
A_2	-0.0046	**A2'**	-0.00175	**S**	52.819
x_o	114.062	**x_o'**	120.9934	**y_0**	-76.68 E6
dx	3.65526	**dx'**	2.4593		
T	Temperature (°C)				

The modulus of elasticity of the HDPE film can be represented by an exponential fitting curve in Fig. 3 and has been extracted by [11]. All fitting parameters have been included in Table 1. Again, all necessary parameters are presented in Table 1, for replication purposes.

$$E_{(T)} = B_1 e^{-(T/s)} y_0 \qquad (5)$$

The modulus of elasticity drops significantly as the temperature increases. Near 120-125 ^oC the material reaches the melting point and we assume that the modulus riches very low values, almost nullified. However, we should stress that at this stage, the material shrinks significantly (shrinkage effect), but cannot hold any applied forces, Fig. 2.

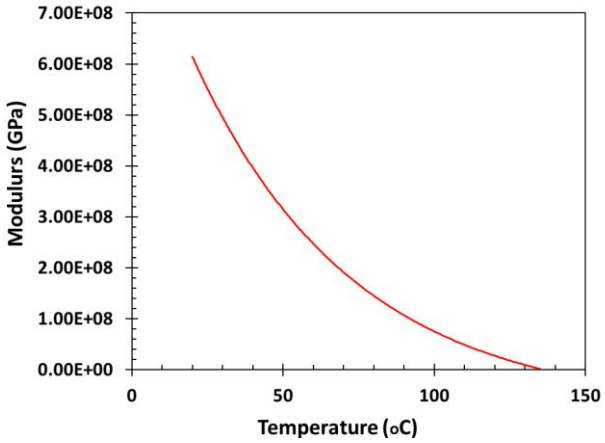

Figure 3: Modulus of elasticity of the HDPE film as a function of temperature [11].

2.3. Numerical modelling details

For the simulation of the experimental campaign, the Abaqus Standard software was used to solve the coupled thermo-mechanical problem, through steady-state or transient 2D and 3D models. The temperature-independent properties of the materials used are presented in Table 2, while the temperature-dependent $CTE_{(T)}$ and $E_{(T)}$ of the HDPE are imported through tabular data. The experiments show that the bilayer exhibits large displacements and rotations, which are considered for the simulation as geometric non-linearity. The convergence studies based on the steady-state total-displacements-vector for the 2D and 3D problem showed that the aspect ratio of the elements should be kept close to unity, due to the large out of plane displacements and rotations. Quadrilateral reduced integration 8-node coupled thermo-mechanical elements were used for the 2D problem, assuming plane strain conditions (CPE8RHT element name). Plane strain conditions can be assumed, since the behaviour of the specimen does not experience large changes along the crosswise axis.

Table 2. Materials properties for FE modelling.

	Density (kg/m^3)	**Poisson's ratio**	**Thermal Conductivity (W/mK)**	**Specific Heat Capacity (J/kgK)**	**Young's Modulus (GPa)**	**Coefficient of Thermal Expansion (μm/m/K)**
Copper	8960	0.355	398	385	120	16
HDPE	1100	0.4	0.4	1000	Eqs. 5	Eq. 4

Linear 8-node full integration coupled thermo-mechanical elements (C3D8T element name)

were used for the 3D model. All the simulations assumed clamped boundary conditions for specimen, initial temperature of 20 ^{o}C, and earth's gravitational field). We should stress that for simplicity reasons, in the FE models, we did not implement the thin adhesive layer because of its very low thickness, that alters minorly the response of the material.

3 RESULTS AND DISCUSSIONS

3.1. Identification of the minimum curvature radius through parametric FE modelling

To select an efficient HDPE thickness for the 40μm copper, a parametric FE study was implemented in Abaqus for a temperature difference of 30 ^{o}C, for HDPE thicknesses between 25μm and 400μm. To evaluate the results, the radius of curvature is calculated for each HDPE thickness. The performance of the specimen increases when the specimen exhibits larger rotations, meaning that optimal HDPE thickness is achieved for minimum radius of curvature. The results illustrated in Fig. 4 show that for increasing HDPE thickness, the radius of curvature starts decreasing until a certain value and then increases again. This happens because very small thicknesses compared to the copper thickness cannot provide enough bending for the specimen curvature, leading to low performance, demonstrated by the high radius of curvature. On the contrary, much thicker HDPE than the copper thickness leads to very high bending stiffness of the specimen, which the copper is not able to pull out of plane.

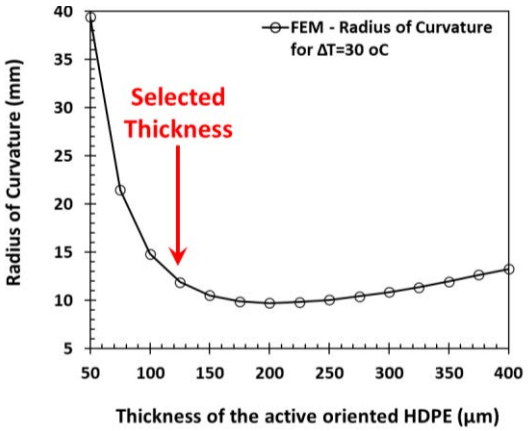

Figure 4: Calculated radius of curvature as a function of the HDPE thickness.

This condition creates large stresses between the material layers, however the bending capabilities are decreased and the radius of curvature is increased. The optimal thickness for the given copper thickness is found around 200μm. However good performance is also observed for thicknesses 125-400μm, as seen in Fig. 4. Solving the well-known analytical equation of bimetallic strip, that has been given by Timoshenko, we observe similar non-linear behaviour. Given the commercially available HDPE thicknesses, a 125μm thick film was selected.

3.2. Plane strain FE modelling and validation

To test the actuator bending capabilities, an experimental campaign was implemented. The proposed actuator consists of highly oriented 125μm thick HDPE and a conductive 40μm copper network. Fig. 5 illustrates two actuators in their initial temperature state at ambient

temperature (Fig. 5A), an intermediate state at approximately 27.5 ^{o}C temperature difference (Fig. 5B), and their final maximum curvature at approximately 62 ^{o}C temperature difference (Fig. 5C). Their change in shape occurs due to the increasing temperature, when a potential difference applied to the copper network leads to the Joule heating effect. The CTE mismatch combined with the relatively stiff HDPE in low temperatures leads to the large curvature of the specimen, as shown in Fig. 5B and C. When the application of the potential difference stops, the temperature of the materials decreases and tends to reach the ambient temperature, making the actuator to return to its original shape.

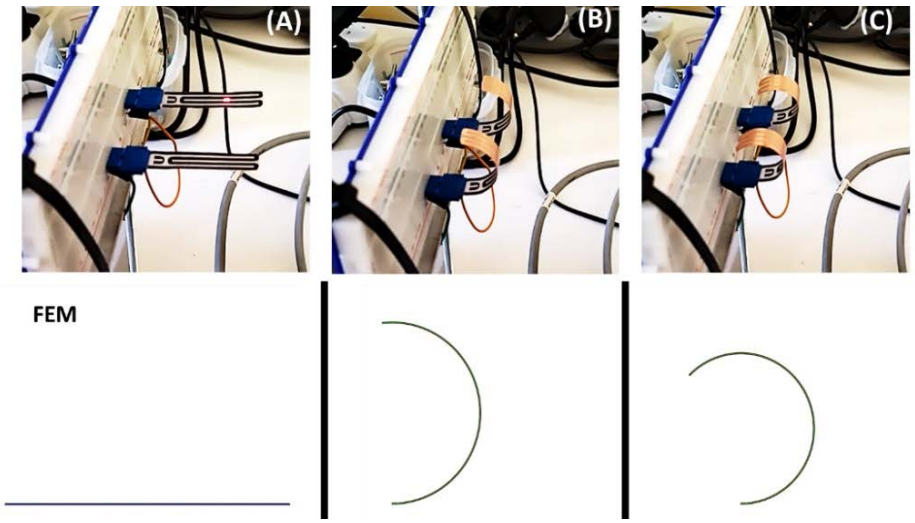

Figure 5: Representation of the soft actuators' capabilities and 2D plain-strain predictions.

To evaluate the experimental results with a 2D plane-strain FE model, the actuator was tested into an apparatus with uniform and controlled temperature. In this way, a steady state condition of the actuator is achieved for each temperature level and compared with the same temperature levels in the FE model. The material properties used in the models are shown in Table 2. Also, perfect contact is assumed between the two materials. Fig. 5A-C illustrate the predicted actuator curvature (FE) at the same temperature differences as the experiment, showing satisfying agreement. For a better comparison of the FE models with the experimental results, the specimen curvature is measured using two metrics: I) the radius of curvature, and II) the transversal displacement, 17mm from the specimen fixed end, using a high precision laser. To compare with the simulation results, these metrics were computed using three FE models, each with the three measured CTEs curves (Fig. 2A, B).

In Fig. 6 the experimental and computational results of the metrics are illustrated as red dots and black lines, respectively. The radius of curvature (Fig. 6A) is progressively decreased for increasing temperature until 75 ^{o}C, exhibiting large out-of-plane deformation. Although the HDPE CTE remains roughly constant (Boltzmann fitting) for this temperature span, the phenomenon is non-linear and tends to reach a certain threshold. This happens due to the

progressively decreasing CTE bending stiffness, due to the decreasing Young's Modulus. The transversal displacement (Fig. 6B) is increasing, non-linearly, for increasing temperature difference up to until approximately 20 ^{o}C, also demonstrating the out-of-plane deformation. For higher temperature levels, the curvature of the specimen is so large that the transversal displacement is no longer measurable. The results of both figures demonstrate that the FE model can accurately describe the large displacements and rotations phenomenon.

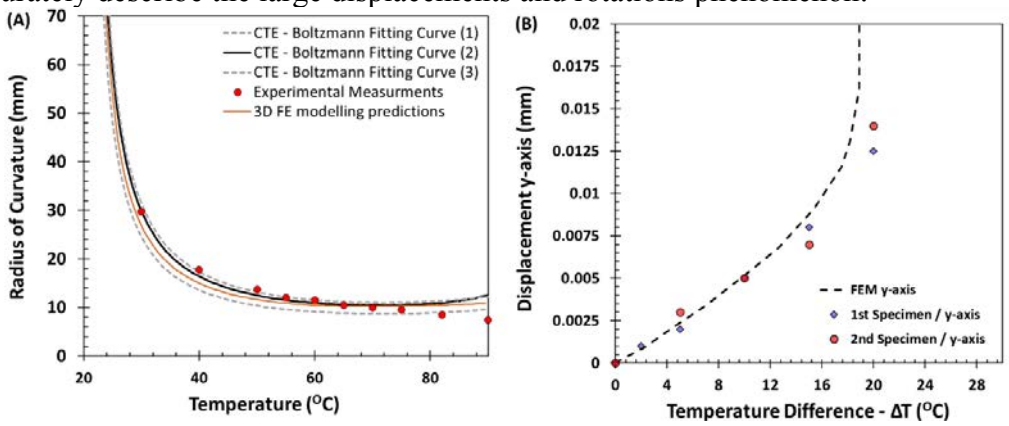

Figure 6: (A) Calculated radius of curvature as a function of temperature (2D and 3D modelling) and comparison with experimental measurements, (B) Calculated and measured displacement of a specific point on the y-axis.

3.3. 3D FE-modelling and validation

Fine mesh 3D FE models were created (Fig. 7A,B) and tested for better prediction of the actuator behaviour, incorporating the anisotropic CTE of the oriented HPDE, which leads to different displacements in the 2-principal axes. In this way, we examine if the final geometry of the specimens differs from the plane strain approach. Fig. 7 illustrates the temperature field on the specimen in the very early stages of the Joule heating effect, when the copper network experiences high temperature (red colour), and the temperature tends to spread to the HPDE. The very fine mesh can be observed in the same time frame in the area of the upper copper network (detail of Fig. 7).

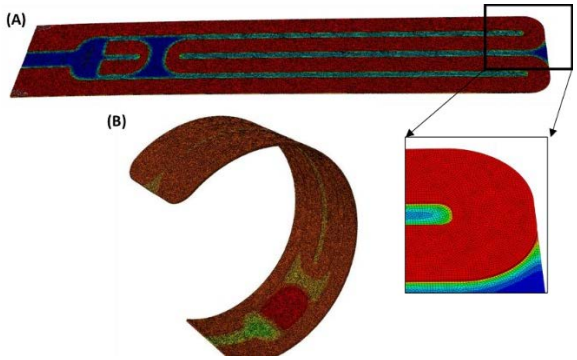

Figure 7: Detailed 3D modelling of the electro-thermo-mechanical problem using temperature depended material properties.

To compare with the experimental results and the 2D plane strain FE model, a steady state temperature level is applied on both planes of the 3D mode, and Fig. 7A,B illustrate the predicted actuator deformation for temperature difference applied in the experiment. It is observed that the curvature is closer to the experimental result, however the discrepancies with the 2D model are insignificant. Thus, we will use the 2D plane-strain FE model for further predictions of the actuator performance and for testing its sensitivity to temperature and time, saving valuable computational cost and time, compared to the 3D model. We should stress that actuators with different dimensions may present very different shape changes and the 3D model is essential.

3.4. Preliminary response measurements as a function of electrical power

The behaviour of the actuator is studied in room temperature conditions when DC voltage is applied to the copper network and the Joule heating effect occurs. For the experiment, the time that the actuator achieves steady state conditions, and the transversal displacement 17mm from the specimen fixed end, are measured for four different power levels, Fig. 8. The steady state conditions occur when the natural convection reaches the same value as the Joule heating power and a temperature equilibrium is reached. For each power level in Fig. 8A, at some point during the experiment the power is turned off, and the actuator returns to its original position due to natural heat convection. Regarding the actuator radius of curvature, it is observed that it is non-linearly correlated with the applied power, Fig. 8B.

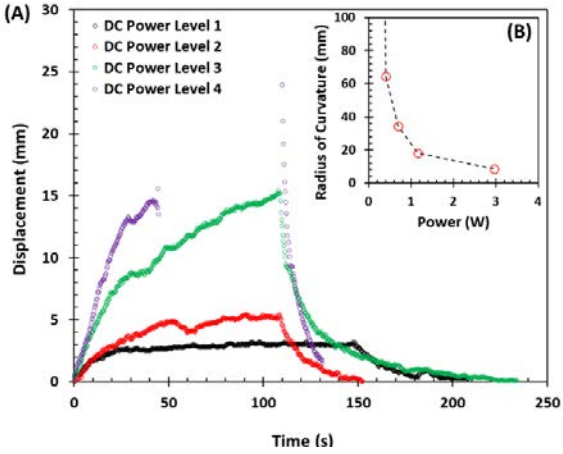

Figure 8: (A) Experimental measurements of the actuator response (transversal displacement of a specific point) as a function of time, for different electrical power levels, (B) Radius of curvature as a function of power.

Both lower power levels lead to curvature where the transversal displacement can be measured for whole experiment, whereas the higher power levels result to curvature where the laser dot is lost at some point and found again when the voltage stops and the natural convection leads the actuator to lower curvature. It is finally noted that the DC power levels are the measures of the total applied power, and the power that is dissipated in the wires and the contacts is not excluded.

3.5. Prediction of the sensitivity using ideal FE models

To evaluate the performance of the actuator as a function of temperature, the 2D model is simulated with applied Joule heating in the copper network and natural convection with air. The temperature-dependent convection coefficient for the upper and lower face of the actuator are calculated and imported in the FE model, as shown in Table 3.

Table 3. Convection coefficients (h) as a function of temperature for the downward, upward surfaces (or in vertical position) of the actuator.

	Temperature (°C)	20	30	40	50	60	70	80	90	100
Horizontal Plane	Downward	0	5.1	6.1	6.7	7.2	7.5	7.9	8.1	8.4
	Upward	0	10.3	12.2	13.4	14.4	15.1	15.8	16.3	16.8
Vertical Plane	Each side	0.4	5.7	6.7	7.3	7.8	8.2	8.5	8.8	9.1

The actuator curvature is quantified by its angle θ, which is defined as the angle between the horizontal line (initial plane of the specimen) and the line that is formed if we unite the fixed end of the specimen with its free end at each temperature level. The actuator sensitivity to temperature change is shown in Fig. 9, as $\Delta\theta/\Delta T$. The actuator illustrates that its temperature sensitivity starts from high values, which gradually decrease as the temperature continues to increase. This means that the actuator is able to produce really high rotations for small changes in temperature (above 20 °C for ΔT=5 °C) but needs higher power for producing larger rotations. This variable sensitivity occurs due to the temperature-dependent material properties of the HDPE (CTE and Young's Modulus).

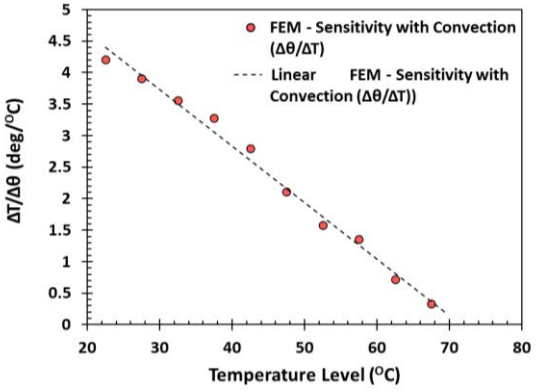

Figure 9: Sensitivity of the actuator as a function of temperature.

Moreover, in order to predict the ideal response of the actuator using FE models, four different power levels were applied to the 2D-plain strain model, Fig. 10A. Figure 10B shows the non-linear correlation of the radius of curvature with the applied power, similarly to the experimental results. To quantify the curvature in the FE model, the angle θ is demonstrated in Fig. 10A, and for each power level, the power is turned off, and the actuator returns to its original position due to natural heat convection.

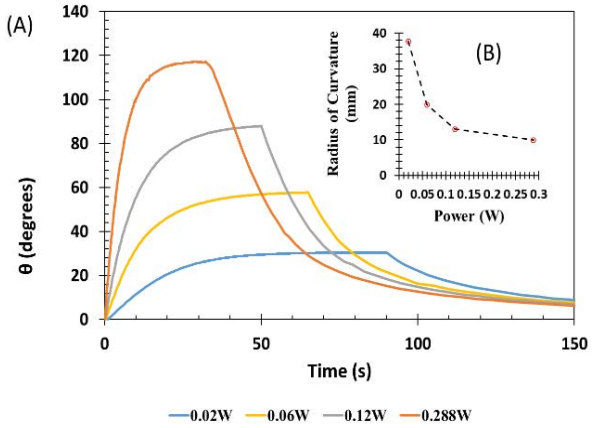

Figure 10: (A) Response of the actuator as a function of time for different electrical power levels, using FE models, (B) Calculated radius of curvature as a function of power.

3.6. 2D modelling of a gripper for object lift: a case study

As a potential application of the proposed electrothermal soft actuator, a preliminary demonstration of two actuators lifting a small rectangular object (e.g., a microchip) is illustrated in Fig. 11. We apply a voltage difference to the copper network of the actuators and natural air convection on vertical planes (Table 3). The rectangular object (density of the object = 1000 kg/m^3) is initially placed on a support at room temperature, Fig. 10A. The temperature of the actuators increases leading to their out-of-plane movement/deformation, and the progressive lift of the plate, Fig. 10B. The final state of this case-study is shown in Fig. 10C. It is observed that the curvature of the actuators is affected by the presence and lifting of the object, because of the mutual interaction, leading to a different deformed shape, compared to a load-free actuator.

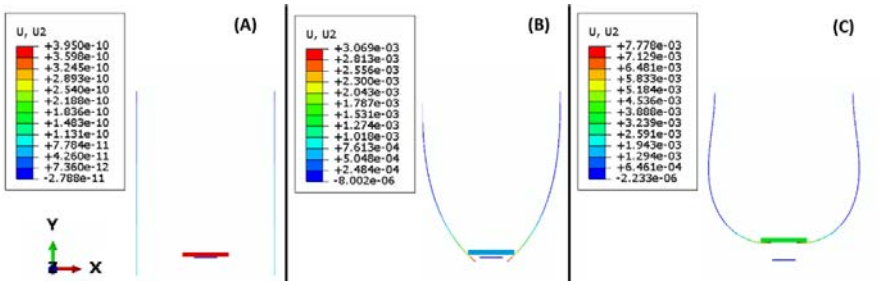

Figure 11: FE modelling of grippers (proposed soft actuators) at different time instances, lilting a rectangular object.

4 CONCLUSIONS

The evaluation and performance of a novel lightweight actuator is presented in this paper, comprising of a highly oriented HDPE and a conductive copper network. The CTE mismatch leads to the large out-of-plane deformation of the actuator, which could be suitable for various applications. An experimental campaign was followed to find the HDPE temperature-dependent CTE and Young's Modulus. These properties were used for the selection of the appropriate HDPE thickness which yields the highest deformation, through a parametric FE

analysis. Also, through an experimental campaign using a specific film thickness was followed to evaluate the performance of the proposed actuator, revealing its great activating potential. The experimental results are compared to 2D FE models (assuming plane strain conditions) and 3D FE models, showing great agreement. The temperature sensitivity was investigated, showing that the actuator response is high for initial temperature changes and decreases almost linearly with time. Finally, an application of the proposed technology is showcased, where two soft actuators effectively lift a rectangular object.

ACKNOWLEDGEMENTS

This research is funded and implemented through the *"H.F.R.I. Research Projects to Support Post-Doctoral Researchers, Greece",* under the name INTEGRAL with project ID: 7401 and Reference Number 49597 - 24/05/2022.

CONTRIBUTIONS

The manuscript was written by N. A. and G. C. The overall methodology and the experiments were conducted by N. A. The thermomechanical FE models were formulated from G. C. Data analysis were conducted from both researchers. N. A. fabricated the actuators.

5 REFERENCES

[1] C. Dawson, J.F.V. Vincent and A.-M Rocca, How pine cones open, *Nature*, 390, 668, 1997.

[2] Y. Hao, S. Zhang, B. Fang, F. Sun, H. Liu & H. Li, A Review of Smart Materials for the Boost of Soft Actuators, Soft Sensors, and Robotics Applications, Chinese Journal of Mechanical Engineering, 35 (37), 2022.

[3] S. Wei and T.K. Ghosh, Bioinspired Structures for Soft Actuators, Advanced Materials Technologies, 7, 2101521, 2022.

[4] R. M. Erb, J. S. Sander, R. Grisch, A. R. Studart, Self-shaping composites with programmable bioinspired microstructures*, Nature Communications*, Vol. 4, 1712, 2013.

[5] S. Gladman, A., Matsumoto, E. A., Nuzzo, R. G., Mahadevan, L. & Lewis, J. A. Biomimetic 4D printing. Nat. Mater. 15, 413–8 (2016).

[6] Q. Zhao, W. Zou, Y. Luo and T. Xie, Shape memory polymer network with thermally distinct elasticity and plasticity, *Science Advances,* Vol. 2(1), e1501297, 2016.

[7] N. Athanasopoulos and N.J. Siakavellas, Bioinspired Temperature-Responsive Multilayer Films and Their Performance under Thermal Fatigue, Biomimetics 2018, 3(3), 20.

[8] Y. Tian et al., Recent Progress of Soft Electrothermal Actuators, Soft Robotics, 8(3), 2021.

[9] N. Athanasopoulos & N. J. Siakavellas, Smart patterned surfaces with programmable thermal emissivity and their design through combinatorial strategies, *Scientific Reports*, 7, 12908, 2017.

[10] N. Athanasopoulos & N. J. Siakavellas, Variable emissivity through multilayer patterned surfaces for passive thermal control: preliminary thermal design of a nano-satellite, 48th International Conference on Environmental Systems, 8-12/06,2018, Albuquerque.

[11] N. Merah et. al, Temperature and loading frequency effects on fatigue crack growth in HDPE pipe material, Arabian Journal for Science and Engineering ,31(2):19-30, 2006.